Decoding peripheral saccade targets from foveal retinotopic cortex

Authors and Affiliations

Luca Kämmer[1,2,3]*, Lisa M. Kroell[3], Tomas Knapen[4,5,6], Martin Rolfs[3,7,8,9], Martin N. Hebart[1,2,10]

[1]Vision and Computational Cognition Group, Max Planck Institute of Human Cognitive and Brain Sciences
[2]Department of Medicine, Justus Liebig University Giessen, Giessen, Germany
[3]Department of Psychology, Humboldt University Berlin, Berlin, Germany
[4]Spinoza Center for Neuroimaging, KNAW Netherlands
[5]Computational Cognitive Neuroscience and Neuroimaging, Netherlands Institute for Neuroscience
[6]Experimental and Applied Psychology, Vrije University Amsterdam, Netherlands
[7]Berlin School of Mind and Brain, Humboldt University Berlin, Germany
[8]Exzellenzcluster Science of Intelligence, Technical University Berlin, Germany
[9]Bernstein Center for Computational Neuroscience Berlin, Germany
[10]Center for Mind, Brain and Behavior, Universities of Marburg, Giessen, and Darmstadt, Germany
*Correspondence: kaemmer@cbs.mpg.de

Highlights

- Saccade targets decodable from foveal early visual areas without foveal stimulation.
- Decoding accuracy is affected by stimulus shape, not semantic information.
- Peripheral stimuli are foveally represented similarly to direct foveal stimuli.
- Intraparietal sulcus activity is consistent with mediation of foveal feedback.

Summary

Human vision is characterized by frequent eye movements[1]. This causes continuous shifts in visual input, yet visual perception appears highly stable[2–4]. A potential mechanism behind this stability is foveal prediction, involving feedback from higher cortical areas during saccade preparation.[5,6] However, it remains unknown (1) whether information is fed back to early visual areas, (2) whether feedback is specific to stimulus features, and (3) which brain regions mediate this effect. To dissociate neural processes associated with stimulus presentation from those related to foveal feedback, we designed a gaze-contingent fMRI paradigm, where saccade targets are removed before they can be foveated. To determine the content of the neural representation, we used natural images as saccade targets and independently manipulated object shape and category. Multivariate analyzes revealed reliable decoding of stimuli from foveal retinotopic areas as early as V1, even though the

stimulus never appeared in the fovea. Decoding was sensitive to shape but not semantic category, indicating that only low-to-mid-level information is fed back. Cross-decoding to a control condition with foveal stimulus presentation yielded reliable decoding, indicating a similar neural representation between foveal feedback and direct stimulation. Eccentricity-dependent analyzes showed a u-shaped decoding curve, confirming that these results are not explained by spillover of peripheral activity or large receptive fields. Moreover, fluctuations in foveal decodability correlated with activity in the intraparietal sulcus, a candidate region for driving this foveal feedback. These findings go beyond trans-saccadic remapping[7,8] by suggesting that peripheral saccade targets are encoded in the foveal cortex in a feature-specific representation[5].

Keywords

visual neuroscience • foveal feedback • fMRI • decoding • retinotopy • saccadic eye movements

Results

Given the fast time-scale of saccade-related processes, it is challenging to investigate foveal feedback using fMRI. To address this challenge and dissociate neural processes elicited by direct visual input from those related to foveal feedback, we designed a gaze-contingent functional MRI study where the saccade target was removed before it could reach the central 2 dva of the fovea (1 dva radius), from which we decoded. To maximize statistical power, we implemented this paradigm using a block-design (Figure 1A). During a block, participants fixated a fixation point until a stimulus appeared in the periphery, cueing them to execute a saccade toward the stimulus. As soon as their gaze came within 6.5 dva of the saccade target, the stimulus disappeared, ensuring that no part of the stimulus ever appeared in the central 2 dva of the fovea. On subsequent trials of the block, the same stimulus appeared in the participant's periphery to cue another saccade, a process which was repeated until the end of a block. While the fovea is commonly defined as the central 5 dva of the visual field[9–11], we focused here on the central part of the fovea, commonly referred to as the foveola[12,13], within 2 dva (1 dva radius), to avoid any overlap of the stimulus and the area from which we decoded. This narrow definition also allowed for enough space to execute a saccade without the stimulus breaching this region. Figure 1C shows that this paradigm was successful in preventing the target from reaching the central 2 dva of the fovea in 99.27% of saccades. All blocks in which the target could have appeared in this region were removed from further analysis (see methods section quantification and statistical analysis).

To compare the experimental condition to activation elicited by direct foveal input, we included a control condition in which participants were instructed to fixate a point at the center of the screen, with the stimulus appearing directly in the center of the fovea (Figure 1A, bottom). To keep visual stimulation frequency comparable, the timing of stimulus appearance and disappearance was recorded for each participant in the experimental condition and replayed in the control condition. To elucidate the content of the stimulus information fed back to foveal retinotopic areas, we used four different natural stimuli (one stimulus per block) allowing us to disentangle the nature of the representation in the foveal retinotopic cortex (Figure 1B). The stimuli were manipulated to match in either shape (horizontal vs. vertical) or semantic category (animals vs. instruments).

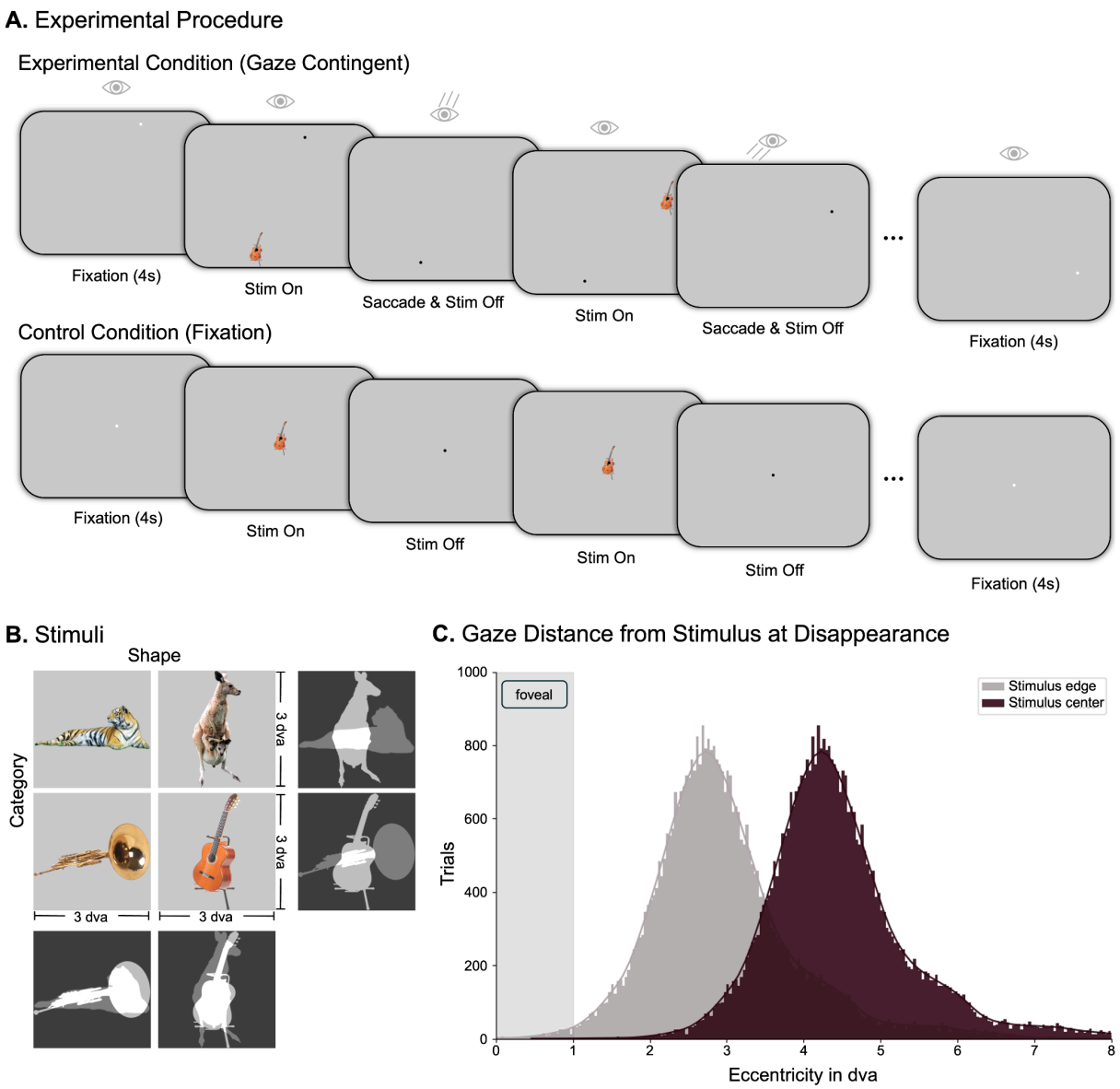

Figure 1. Experimental setup (A) Illustration of one block of the experimental and control conditions, respectively. During each block in the experimental condition, a peripheral saccade target was shown, which participants were instructed to fixate. The target disappeared before it could be foveated, and once fixation was achieved, a new target appeared, until the block was over (duration: 11 seconds). The timing of target appearance and disappearance from the experimental condition was recorded and used in the control condition, where targets appeared at fixation. (B) Depiction of the 4 stimuli used in the experiment, which were matched in either visual shape (horizontal / vertical) or semantic category (animal / instrument). Each stimulus appeared equally often in both conditions. (C) Histogram of the gaze distance from the stimulus right after stimulus disappearance including all trials. The blocks in which the stimulus edge may have appeared in the participants' fovea during at least one saccade were excluded. More detailed eye tracking results are reported in Figure S2.

Decoding foveal feedback

To test for the presence of stimulus-specific activation in foveal regions of early visual cortex, we used cross-validated multivariate decoding[14], which reveals information that allows discriminating between different stimuli. We compared all pairs of stimuli in the experimental and control condition, respectively (chance level: 50%). In the experimental condition, we found above chance decoding in central foveal V1 ($t(27) = 8.81$, $p < 0.001$, mean = 57.43%) (Figure 2A). This result demonstrates that information about the peripheral saccade targets is present in central foveal regions of V1, despite never appearing in the corresponding part of the fovea. To compare this finding to direct foveal stimulus presentation, we repeated the same analysis for the control condition, where we also found strong significant decoding ($t(27) = 19.92$, $p < 0.001$, mean = 84.06%) (Figure 2A). To further examine the nature of the neural representation elicited by foveal feedback, we cross-decoded from experimental to control trials by training a classifier on data from central foveal V1 in the experimental condition and testing it on the control condition. Decoding was significantly above chance ($t(27) = 5.22$, $p < 0.001$, mean = 57.2%), indicating a similar representational format between the neural representation elicited by direct presentation of the stimulus in the fovea and that elicited by foveal feedback (Figure 2A).

This pattern of results may alternatively be explained by spillover from peripheral regions or large receptive fields in the fovea reaching into the periphery[15]. To address this issue, we investigated decoding as a function of eccentricity in early visual regions (Figure 2B). Foveal decoding due to peripheral spillover would predict a monotonic relationship between peripheral and foveal decoding in the experimental condition. Instead, we found a u-shaped relationship, with stronger decoding from peripheral and foveal regions compared to parafoveal regions. These results highlight the spatial pattern of foveal feedback, separating decoding due to direct stimulus presentation in the periphery and decoding due to feedback to foveal regions. As expected, in the control condition, decoding was the highest in the center of gaze and dropped off towards the periphery.

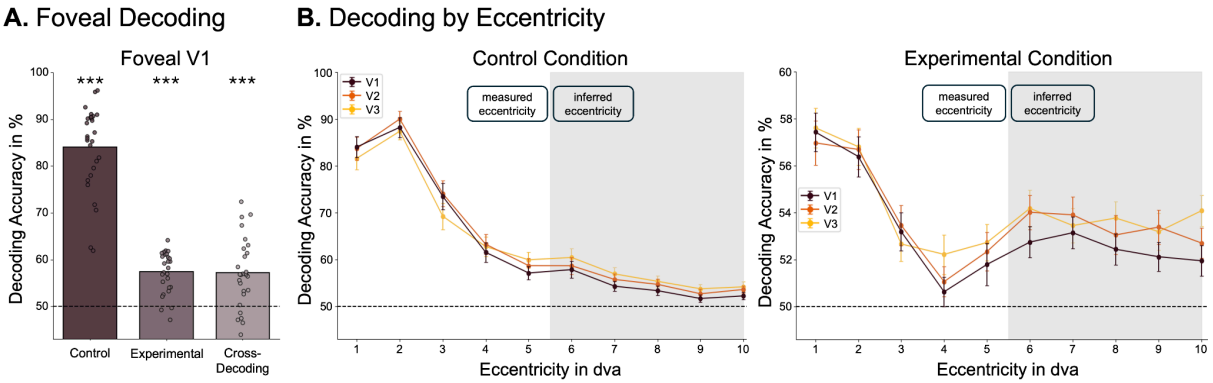

Figure 2. Foveal feedback can be decoded from V1 (A) Average decoding accuracy over all pairwise comparisons for control and experimental conditions and for cross-decoding from experimental to control condition. (B) Average decoding accuracies for all early visual areas as a function of eccentricity for both experimental and control conditions. Error bars represent standard error of the mean. Note that the graphs have different scales of decoding accuracy. The central eccentricities (1-5 dva) were measured using a retinotopic localizer, the outer ones (6-10 dva) were inferred from structural data using Neuropythy[16].

Foveal feedback is sensitive to stimulus shape, not semantic category

Our use of natural stimuli allowed us to test the effects of shape and category on decoding accuracy to better understand the nature of the information fed back to foveal areas (Fig. 3A). Decoding was assessed between visually similar yet semantically dissimilar stimuli (across category), between semantically similar yet visually dissimilar stimuli (across shape), and between visually and semantically dissimilar stimuli (across both). The latter comparison served as a baseline, assessing how good decoding is for maximally different stimuli.

A similar pattern of decoding accuracies emerged in both experimental and control conditions: Decoding from foveal V1 across category dropped significantly relative to baseline (experimental condition: $t(27) = 2.25$, $p = 0.033$, difference = 3.03%; control condition: $t(27) = 14.74$, $p < 0.001$, difference = 16.64%), while decoding across shape remained high (Fig. 3B). This pattern indicates that the nature of the feedback signal in the experimental condition was related to stimulus shape information and not semantic category. The fact that the overall pattern of results across conditions looks similar in the experimental and control conditions is in line with the notion that direct stimulus presentation and foveal feedback elicit similar neural representation, as suggested by the cross-decoding results described above (Fig. 2A). To test the degree to which the classifier was able to pick up on category

information, we repeated the same analysis in the lateral occipital area (LO), which has been shown to capture higher level information about object category[17]. In this area, the pattern was reversed: Decoding dropped across shape relative to baseline (experimental condition: $t(27) = 3.41$, $p = 0.002$, difference = 5.31%; control condition: $t(27) = 7.25$, $p < 0.001$, difference = 6.7%), while it remained high across category, which suggests that this activation more strongly reflects information about the semantic category than stimulus shape.

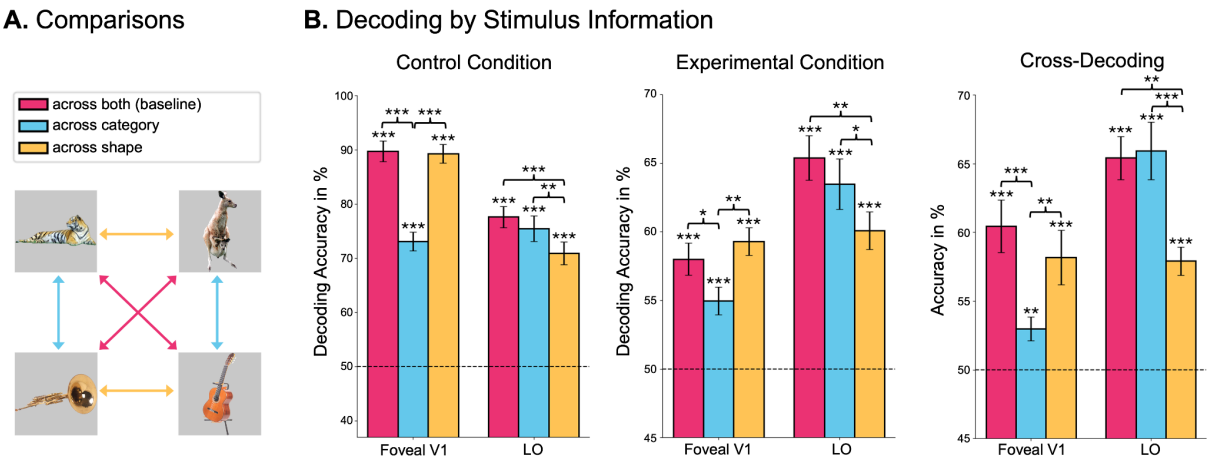

Figure 3. Foveal feedback is sensitive to stimulus shape, not semantic category (A) Schematic depiction of comparisons to assess the information content of the neural representations. Comparisons across category assess similarity of representations in terms of visual stimulus properties, with lower decoding accuracies indicating coding for visual information. Similarly, comparing across shape assesses categorical information. Comparing across both serves as a baseline, showing how high decoding accuracy is between maximally different stimuli. (B) Decoding accuracies for all comparisons using data from foveal regions of V1 and from the lateral occipital area (LO). Note that the graphs have different y-axes of decoding accuracy. Split decoding accuracies for all early visual areas are reported in Figure S1.

The role of IPS in mediating foveal feedback

While the previous analyzes revealed the pattern of foveal feedback in early visual regions, they left open which neural regions might be involved in driving or mediating this effect. To this end, we conducted an exploratory analysis looking at the block-by-block fluctuations in foveal decodability in the experimental condition. As a measure of decodability, we used the continuous decision value of the classifier, which signifies the distance to the classifier's hyperplane on a given trial. Using a parametric modulation analysis, we explored which brain region's activity

increased or decreased as a function of foveal decodability. To control for the effects of the direct peripheral presentation of the stimulus, we used the block-by-block fluctuations of peripheral decoding in the experimental condition as a baseline.

Since foveal feedback is a process tightly linked to saccadic eye movements[5], we hypothesized that regions associated with eye movements are most likely involved in driving this effect. We focused on three regions that have consistently been associated with eye movements and object representations: Frontal eye fields (FEF)[18,19], intraparietal sulcus (IPS)[20,21], and lateral occipital area (LO)[22] (Figure 4A). Not all voxels in these regions were expected to be functionally active. Therefore, to focus analyzes on the most relevant voxels, we selected the 100 voxels in each of these regions that activated most strongly in the experimental condition in general. The region of interest (ROI) analyzes showed that all of these areas were significantly related to both foveal and peripheral decoding in the experimental condition (Figure 4B). Specifically, IPS showed significantly larger activation related to foveal decoding compared to peripheral decoding ($t(27) = 2.53$, $p = 0.009$, difference = 4.22), suggesting that IPS may be involved in foveal feedback. While effects in the other regions went in the expected direction, they remained non-significant after correcting for multiple comparisons (LO: $t(27) = 0.67$, $p = 0.256$, difference = 0.53; FEF: $t(27) = 2.07$, $p = 0.024$, difference = 1.98).

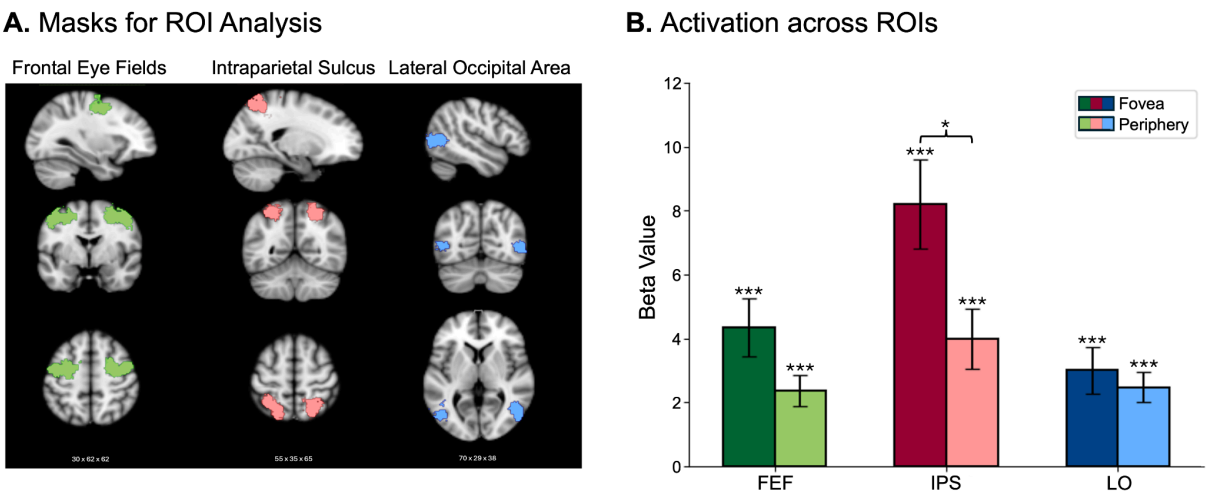

Figure 4. Correlation of foveal decoding with ROI activation (A) Cortical masks used in the ROI analyzes. These masks were generated using Neurosynth[23] with the keyword "eye movements". For later analyzes, only the 100 most activating voxels were selected in each area. (B) Results of the ROI analyzes comparing neural activation as a function of foveal and peripheral decoding in three key areas related to eye movements. It showed significantly higher activation in the IPS in association with foveal, compared to peripheral decoding.

Discussion

The present preregistered study provides evidence that early foveal retinotopic areas are involved in the processing of peripheral saccade targets, even if the stimuli are never presented in the central part of the fovea. Using a combination of fMRI and eye-tracking, we were able to decode the identity of saccade targets from foveal regions of early visual cortex (Fig. 2A), suggesting that shape-specific information about peripheral targets is fed back to foveal areas during saccade preparation. We also showed that this foveal feedback is unlikely to be caused by spillover from peripheral regions (Fig. 2B) and that it has a similar neural representation as direct stimulus presentation, as shown by the above chance cross-decoding (Fig. 2A). This cross-decoding alleviates concerns about the type of information picked up by the decoder in the experimental condition. That is, it cannot be explained by the decoder picking up small changes in eye movements between different stimuli[15], since the representation - at least in part - transfers to the control condition, where participants did not move their eyes. Furthermore, we showed that foveal feedback is sensitive to the shape, but not the semantic category of the stimulus (Fig. 3B), which suggests that foveal feedback in early visual cortex is rather rudimentary and does not convey a category-invariant stimulus representation. Lastly, in an exploratory analysis, we identified the intraparietal sulcus (IPS) as a candidate region for driving foveal feedback (Fig. 4B).

Saccadic remapping or foveal prediction

Saccadic remapping, that is, the increase of activity of neurons in anticipation of a stimulus entering their receptive field, has been observed all over the visual cortex[2,24,25]. These shifts of activity are commonly viewed as a predictive remapping of attention pointers, which do not themselves contain information about the content of the stimulus[7,26,27]. Foveal prediction, on the other hand, goes beyond a purely attentional effect and instead contains content-specific information about the saccade targets. Kroell and Rolfs[5] in their psychophysical experiments found that during saccade preparation, peripheral saccade target representations were enhanced in the pre-saccadic fovea. These findings led the researchers to conclude that the fovea plays a unique role in maintaining perceptual continuity by predicting future inputs during saccade preparation. Our results support this view by showing

shape-sensitive decoding, as well as the cross-decoding results from the experimental to control condition, indicating that foveal feedback may lead early foveal regions to share features with the peripheral target stimulus in anticipation of an upcoming saccade. These findings provide another indication for the distinction between saccadic remapping and foveal prediction, although more research is needed to differentiate these effects across the visual field.

Comparing foveal feedback to direct presentation

The present study supports a predictive account of foveal processing[5] and further characterizes the nature of this effect. The decoding patterns revealed that the information about the saccade targets that is fed back to the foveal cortex may reflect shape information, but does not contain higher-level categorical information. These decoding patterns resemble the ones we found in the control condition, where the stimuli were presented directly in the fovea (Fig. 3B). Lastly, it was possible to cross-decode by training a decoder on foveal V1 data from the experimental condition and decoding stimulus identity from the same regions in the control condition at above chance-level (Fig. 2B). These findings suggest shared representational formats in early visual areas between foveal prediction and direct stimulus presentation, which indicates that foveal feedback reflects both spatial and basic shape features of the target similarly to the direct presentation of the stimulus.

IPS as a candidate modulator of foveal prediction

In a parametric modulation analysis, we found that the intraparietal sulcus (IPS) was significantly more active in association with foveal decoding compared to peripheral decoding in the experimental condition (Fig. 4B). This area has been described as neither a strictly visual nor motor area but instead as performing visuomotor integration functions, such as determining the spatial location of saccade targets and forming plans to make eye movements[20,21]. Further research has shown that this region represents salient stimuli, relative to the center of gaze[28]. This integrative function makes the IPS an ideal candidate for modulating feature-specific feedback to foveal areas during saccade preparation. While this analysis is exploratory, it offers yet another indication that foveal feedback is inherently linked to saccadic eye movements, and that IPS could play an important role in driving this

effect. Future hypothesis-driven research could specifically target this region to more clearly determine its role in foveal feedback.

Limitations and future directions

Despite the insights gained in the present study, several open questions remain. We did not specifically test if we can find foveal feedback from peripheral targets without any stimulus-specific task (e.g., no eye movements), which is relevant to showing that foveal feedback is task-dependent. However, similar control conditions have been run by Williams et al.[15] and Knapen et al.[6]. Neither found any stimulus-specific foveal activation with peripheral target presentation in the absence of a specific task. To further separate the results laid out in this study from the process of saccadic remapping, future studies could specifically test periphery-to-periphery feedback for feature-specific activation. Additionally, while the stimulus-specific effects reported in the present study were robust, the results were limited to 4 different stimuli, since the addition of further conditions would have led to a reduction in statistical power. Future studies could expand upon the present approach by increasing the number of stimuli, possibly collecting data across multiple sessions to achieve sufficiently large effects. While these questions offer exciting research avenues for future studies, our results demonstrate the importance of foveal feedback during saccadic eye movements, offering a plausible candidate mechanism for our ability to integrate visual information across saccades.

STAR ★ Methods

This study was pre-registered on OSF (https://osf.io/rxacd/), detailing the hypotheses, methodology, and planned analyzes prior to data collection, with the exception of the exploratory parametric modulation analysis.

Key resources table

REAGENT or RESOURCE	SOURCE	IDENTIFIER
Deposited data		
Primary Data	This Paper	https://openneuro.org/datasets/ds005933
Experimental models: Organisms/strains		
Human Participants	Recruited by MPI CBS Leipzig	N/A
Software and algorithms		
Python	Python Software Foundation	https://www.python.org/; RRID: SCR_008394
Custom Python Scripts	This Paper	https://github.com/Lucakaemmer/FovealFeedback.git
fMRIprep	Esteban et al.[29]	https://fmriprep.readthedocs.io/en/20.2.0/workflows.html
FSL	Jenkinson et al.[30]	https://fsl.fmrib.ox.ac.uk/fsl/docs/#/
MATLAB	Mathworks	https://www.mathworks.com/products/matlab.html; RRID:SCR_001622

Resources availability

Lead contact

Further information and requests for resources and reagents should be directed to and will be fulfilled by the lead contact, Luca Kämmer (kaemmer@cbs.mpg.de).

Materials availability

This study did not generate new materials.

Data and code availability

The dataset collected for this study is available on OpenNeuro at https://openneuro.org/datasets/ds005933, the code generated for this analysis is available at https://github.com/Lucakaemmer/FovealFeedback.git.

Experimental model and study participant details

The experiment was performed with human participants recruited by the recruitment system of the Max Planck Institute for Cognitive and Brain Sciences in Leipzig, where the experiment was conducted. 30 participants were tested, which is similar to comparable studies. Two participants were excluded. One person had poor eye-tracking performance, which impaired the functioning of the gaze-contingent aspect of the experiment (fewer than 100 valid saccades in the experiment). The other was excluded based on poor fMRI data, likely due to drowsiness, which made it impossible to generate retinotopic masks. The remaining 28 participants (14 male and 14 female) were 18–40 years old (average 27.54 years), healthy, right-handed, and had normal or corrected-to-normal vision. Participants were compensated with €12 per hour. The experiment was conducted in accordance with the declaration of Helsinki, and the experimental procedure was approved by the ethics review board of the University of Leipzig (reference number: 421/23-ek). The participants gave written informed consent before taking part in the study.

Method details

Stimuli

The stimuli were four different object images taken from the Hemera object dataset (H. Technologies. Hemera photo objects). These stimuli were chosen to match either regarding their visual shape (horn and tiger, guitar and kangaroo) or their semantic category (horn and guitar, tiger and kangaroo). The stimuli that were visually similar were also semantically dissimilar, and vice versa (Figure 1B). All stimuli were normalized regarding their overall luminance and root mean square contrast and were presented at a size of 3 dva.

Behavioral task

In the experimental condition, objects appeared in eight different locations arranged in a circle around the screen, each of them 4º away from the center of the

screen (Figure 1A). Experimental blocks started with a white fixation point appearing in one of these eight locations. After 4 seconds, the fixation point turned black, and one of the four stimuli appeared in one of the three locations on the opposite side of the screen, 7.4º or 8º away from the fixation point. The stimulus only appeared if participants were fixating on the fixation point. Stimulus appearance was the cue for the participant to perform a saccade. As soon as their gaze came within 6º of the stimulus during the saccade, the stimulus disappeared to prevent it from appearing in the participant's fovea. After an inter-trial interval of 0.5 seconds, the same stimulus appeared again at the next location. This pattern repeated for 11 seconds, concluding one experimental block. One run consisted of 20 blocks, switching to a different stimulus in each block. The experiment included 5 experimental runs and 5 control runs.

In the control condition, stimuli were presented at the center of the fovea, with fixation at the center of the screen (Figure 1A). The overall timing of the stimulus presentation was the same as in the experimental condition. To this end, the timing of stimulus appearance and disappearance in the experimental condition, which depended on the participants' eye movements, was recorded and used in the control condition to provide the same exposure duration to the stimulus across conditions.

Lastly, an eccentricity retinotopic localizer and standard object localizer task were used to create retinotopic mapping and to identify object-processing areas in each participant. The retinotopic localizer consisted of six iterations of contracting or expanding rings to map each participant's eccentricity in early visual areas. The object localizer consisted of blocks of either object images or scrambled images to separate object-processing areas from lower-level visual areas.

Imaging

fMRI scanning was performed at the Max Planck Institute for Human Cognitive and Brain Sciences in Leipzig, Germany, using a Siemens Magnetom Skyra 3T scanner equipped with a 32-channel head coil (Siemens, Erlangen). Whole-brain T2*-weighted echo-planar images (EPI) were collected with the following parameters: repetition time (TR) = 2000 ms, echo time (TE) = 23.6 ms, flip angle = 80°, field of view (FOV) = 204mm², voxel size = 2 × 2 × 2 mm³, and 69 transverse slices with no gap. An interleaved slice acquisition was used with a multiband acceleration factor of 3 and no in-plane acceleration, and the phase

encoding direction was anterior to posterior. High-resolution T1-weighted anatomical images were acquired at the end of the scanning session using a standard magnetization-prepared rapid gradient echo (MPRAGE) sequence. Parallel imaging with GRAPPA was utilized for the T1-weighted MPRAGE sequence with an acceleration factor of 2.

For eye tracking, we used an EyeLink 1000+ Eyetracker, sampling the right eye at 1000 Hz. The eye tracker was calibrated using a 13-point setup to ensure high eye tracking quality. The stimuli were presented using a VPixx PROPixx projector, set to a real-time refresh rate of 180 Hz to allow for the gaze-contingent disappearance of the stimulus before participants could fixate it. The presentation was programmed in Python using PsychoPy[31].

Each participant completed one scanning session, starting with 10 experimental runs (5 gaze-contingent and 5 fixation runs), which took 320 s each. The retinotopic localizer run took 206 s, and the object localizer run took 426 s, bringing the overall time inside the MRI scanner to around 80 minutes, including structural scans, breaks, and the calibration of the eye tracker.

Quantification and statistical analysis

The fMRI data were preprocessed using fMRIprep version 20.2.0[29]. Brain surfaces were reconstructed using recon-all from FreeSurfer v6.0.1[32]. Functional data were slice-time corrected using 3dTshift from AFNI v16.2.07[33] and motion-corrected using mcflirt[30]. The functional data used for the decoding analysis remained in each participant's native space, without registering to a brain template.

Univariate analyzes were conducted on all experimental and control runs using FSL's FEAT (v6.00) to perform a general linear model analysis[30]. The resulting beta values for each block were then used in the subsequent multivariate decoding analysis. We chose pairwise classification over multiclass classification (1) since our intent was not to build a classifier for real-world applications but to infer from the presence of above chance accuracies the presence of discriminative information[14] and (2) since most common multiclass classification approaches implicitly rely on the comparison of multiple pairwise classifiers anyway. For the decoding analyzes and statistical tests, a custom-written Python pipeline was used; a linear support vector machine with 5-fold cross-validation was used for decoding, provided by the Python package sklearn[34]. Decoding accuracies were compared with t-tests using the

Python package SciPy[35]. One-sample t-tests were used to assess if decoding accuracies were significantly different from chance. Since a within-subjects design was used in which all participants went through all the conditions, paired, two-sided t-tests were used to compare decoding accuracies (across shape, across category, across both). The significance threshold was set at $p < 0.05$. Significance levels in figures are indicated as follows: $*p < 0.05$, $**p < 0.01$, $***p < 0.001$.

Anatomical masks for V1, V2, and V3 were generated for each participant using Neuropythy[16]. The same package was used to estimate the outer retinotopic eccentricities from 6 to 10 dva. The inner eccentricities from 1 to 5 degrees were estimated using the functional retinotopic localizer. A univariate analysis was used to estimate the voxels responding to a certain range of eccentricity. Similarly, anatomical masks for LO were generated for each participant using the functional object localizer.

The parametric modulation analysis was conducted using FSL's FEAT. Using the decoders' block-by-block fluctuations in decision scores as regressors, the parametric modulation analysis was run on the preprocessed data from the experimental runs, which was converted to MNI space to allow for second-level analyzes across participants. Masks for the eye-tracking ROIs were generated using the website Neurosynth[23], which synthesizes data from thousands of fMRI studies to create functional cortical masks in MNI space. Using the keyword "eye movements", we generated masks of regions known to be associated with eye movements: Frontal eye fields (FEF)[18,19], intraparietal sulcus (IPS)[20,21], and lateral occipital area (LO)[22] (Figure 4A). We then isolated the 100 voxels per area that activated most strongly in the experimental condition overall, independent of which stimulus was shown. Beta estimates for these 100 voxels in each area were then compared with paired, one-sided t-tests using SciPy to test our hypothesis that foveal decoding was associated with larger neural activation in our ROIs. These tests were corrected for multiple comparisons using Bonferroni correction.

To assure that there was no direct foveal stimulation in the experimental condition, we excluded all the experimental blocks in which any part of the stimulus may have appeared in the participants' fovea during at least one saccade, which happened in 0.73% of all saccades. Since entire blocks were removed when they contained a single such saccade, this led to an exclusion of 8.49% of experimental

blocks. To keep the balance between experimental and control conditions, we also excluded the corresponding blocks from the control condition.

The processing of offline eye movement data was performed in Matlab 2018b (Mathworks, Natick, MA, USA). Within an experimental block a trial only started (characterized by the appearance of a stimulus) once participants fixated within 1dva of the initial fixation point, and only ended once they fixated within 1 dva of the target fixation point. In the offline analysis, a saccade was detected when 2D velocity exceeded 5 standard deviations from the median for a minimum of 5ms[36]. Saccade candidates that were less than 10 ms apart (usually resulting from post-saccadic oscillations[37]) were merged into a single saccade. On average, participants performed 1084 (± 206.17) trials over the course of the experiment, which amounts to 10.84 trials per experimental block. Overall, participants reached the target area (within 2 dva of stimulus center) in a single saccade in 76.07% of all stimulus appearances, and in 16.94% in more than one saccade. Note that humans can plan two saccades in advance and still allocate attention to the final goal ahead of the first saccade[7,38–40]. In 6.99% of trials, no saccade was detected in the offline analysis, probably due to tracking noise in the MRI scanner. In the worst case, these trials would only have added noise. Average saccade latency was 240.70 ms, and average saccade amplitude was 6.76 dva. All the figures were prepared using Python and PowerPoint.

Acknowledgements

We would like to thank the members of the Vision and Computational Cognition Group at the Max Planck Institute for Human Cognitive and Brain Sciences for their valuable feedback and contributions to this study. We would also like to thank the staff in the MRI department at the MPI-CBS that supported the data collection. This work was supported by a doctoral student scholarship awarded to L.K. by the German Academic Scholarship Foundation (”Studienstiftung des Deutschen Volkes”), a research group grant by the Max Planck Society awarded to M.N.H., the ERC Starting Grant project COREDIM (ERC-StG-2021-101039712) and the Hessian Ministry of Higher Education, Science, Research and Art (LOEWE Start Professorship to M.N.H. and Excellence Program ‘The Adaptive Mind’). M.R. was supported by the ERC Consolidator Grant project VIS-A-VIS (grant agreement

835715). The funders had no role in study design, data collection and analysis, decision to publish or preparation of the manuscript.

Author contributions

L.K., M.R., and M.N.H. conceived and designed the research. L.K. performed experiments, analyzed the data and prepared figures. L.K. and L.M.K performed eye tracking analyzes. L.K., L.M.K., T.K., M.R., and M.N.H. interpreted the results. L.K. wrote the original draft of the paper. T.K., L.M.K., M.R., and M.N.H. reviewed and edited the paper. M.N.H. oversaw the project.

Declarations of interest

The authors declare no competing interests.

Supplemental information

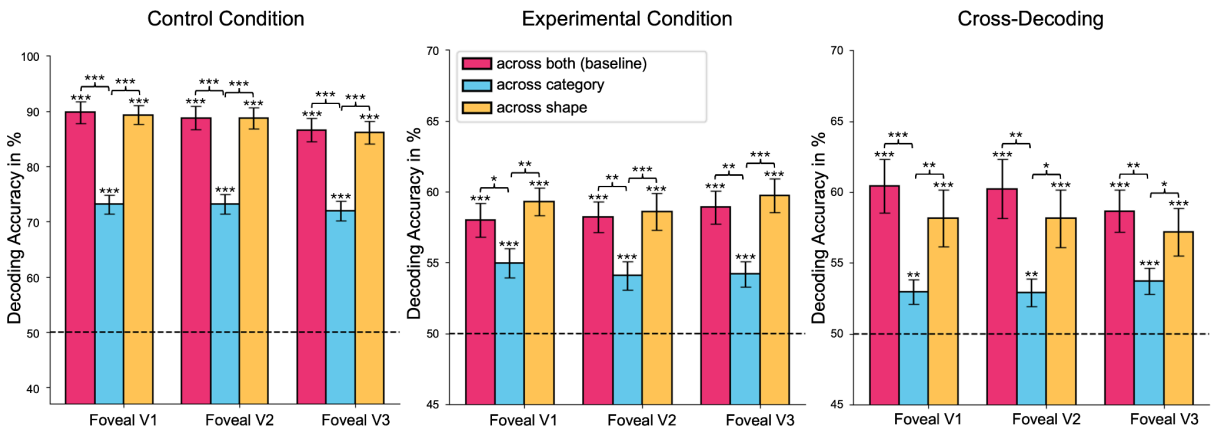

Figure S1. Decoding stimulus content from all early foveal areas. Decoding accuracies for all comparisons using data from foveal regions of V1, V2, and V3. These graphs show that the results from V1 outlined in this publication generalize to other regions of the early visual cortex.

References

1. O'Regan, J.K. (1992). Solving the "real" mysteries of visual perception: The world as an outside memory. *Psychol. Rev.* 99, 463–488. https://doi.org/10.1037/h0084327.
2. Golomb, J.D. & Mazer, J.A. (2021). Visual remapping. *Annu. Rev. Vis. Sci.* 7, 257–277. https://doi.org/10.1146/annurev-vision-032321-100012.
3. Melcher, D. & Colby, C.L. (2008). Trans-saccadic perception. *Trends Cogn. Sci.* 12, 466–473. https://doi.org/10.1016/j.tics.2008.09.003.
4. Burr, D.C., Morrone, M.C. & Ross, J. (1994). Selective suppression of the magnocellular visual pathway during saccadic eye movements. *Nature* 371, 511–513. https://doi.org/10.1038/371511a0.
5. Kroell, L.M. & Rolfs, M. (2022). Foveal vision anticipates defining features of eye movement targets. *eLife* 11, e78106. https://doi.org/10.7554/eLife.78106.
6. Knapen, T., Swisher, J.D., Tong, F. & Cavanagh, P. (2016). Oculomotor remapping of visual information to foveal retinotopic cortex. *Front. Syst. Neurosci.* 10:54. https://doi.org/10.3389/fnsys.2016.00054.
7. Rolfs, M., Jonikaitis, D., Deubel, H. & Cavanagh, P. (2011). Predictive remapping of attention across eye movements. *Nat. Neurosci.* 14, 252–256. https://doi.org/10.1038/nn.2711.
8. Wurtz, R.H. (2008). Neuronal mechanisms of visual stability. *Vision Res.* 48, 2070–2089. https://doi.org/10.1016/j.visres.2008.03.021.
9. Curcio, C.A., Sloan, K.R., Kalina, R.E. & Hendrickson, A.E. (1990). Human photoreceptor topography. *J. Comp. Neurol.* 292, 497–523. https://doi.org/10.1002/cne.902920402.
10. Hendrickson, A. (2005). Organization of the adult primate fovea. In P.L. Penfold & J.M. Provis (Eds.), *Macular Degeneration* (pp. 1–23). Springer-Verlag. https://doi.org/10.1007/3-540-26977-0_1.
11. Hendrickson, A. (2009). Fovea: Primate. In *Encyclopedia of Neuroscience* (pp. 327–334). Elsevier. https://doi.org/10.1016/B978-008045046-9.00920-7.
12. Poletti, M., Rucci, M. & Carrasco, M. (2017). Selective attention within the foveola. *Nat. Neurosci.* 20, 1413–1417. https://doi.org/10.1038/nn.4622.
13. Heckenlively, J.R. & Arden, G.B. (Eds.). (2006). *Principles and Practice of Clinical Electrophysiology of Vision* (2nd ed.). MIT Press. https://doi.org/10.7551/mitpress/5557.001.0001.
14. Hebart, M.N. & Baker, C.I. (2018). Deconstructing multivariate decoding for the study of brain function. *NeuroImage* 180, 4–18. https://doi.org/10.1016/j.neuroimage.2017.08.005.

15. Williams, M.A., Baker, C.I., Op de Beeck, H.P., Mok Shim, W., Dang, S., Triantafyllou, C. & Kanwisher, N. (2008). Feedback of visual object information to foveal retinotopic cortex. *Nat. Neurosci.* 11, 1439–1445. https://doi.org/10.1038/nn.2218.
16. Benson, N.C. & Winawer, J. (2018). Bayesian analysis of retinotopic maps. *eLife* 7, e40224. https://doi.org/10.7554/eLife.40224.
17. Grill-Spector, K., Kourtzi, Z. & Kanwisher, N. (2001). The lateral occipital complex and its role in object recognition. *Vision Res.* 41, 1409–1422. https://doi.org/10.1016/S0042-6989(01)00073-6.
18. Paus, T. (1996). Location and function of the human frontal eye-field: A selective review. *Neuropsychologia* 34, 475–483. https://doi.org/10.1016/0028-3932(95)00134-4.
19. Vernet, M., Quentin, R., Chanes, L., Mitsumasu, A. & Valero-Cabré, A. (2014). Frontal eye field, where art thou? Anatomy, function, and non-invasive manipulation of frontal regions involved in eye movements and associated cognitive operations. *Front. Integr. Neurosci.* 8:66. https://doi.org/10.3389/fnint.2014.00066.
20. Andersen, R.A., Brotchie, P.R. & Mazzoni, P. (1992). Evidence for the lateral intraparietal area as the parietal eye field. *Curr. Opin. Neurobiol.* 2, 840–846. https://doi.org/10.1016/0959-4388(92)90143-9.
21. Andersen, R.A. (1989). Visual and eye movement functions of the posterior parietal cortex. *Annu. Rev. Neurosci.* 12, 377–403. https://doi.org/10.1146/annurev.ne.12.030189.002113.
22. Kawawaki, D., Shibata, T., Goda, N., Doya, K. & Kawato, M. (2006). Anterior and superior lateral occipito-temporal cortex responsible for target motion prediction during overt and covert visual pursuit. *Neurosci. Res.* 54, 112–123. https://doi.org/10.1016/j.neures.2005.10.015.
23. Yarkoni, T., Poldrack, R.A., Nichols, T.E., Van Essen, D.C. & Wager, T.D. (2011). Large-scale automated synthesis of human functional neuroimaging data. *Nat. Methods* 8, 665–670. https://doi.org/10.1038/nmeth.1635.
24. Duhamel, J.-R., Colby, C.L. & Goldberg, M.E. (1992). The updating of the representation of visual space in parietal cortex by intended eye movements. *Science* 255, 90–92. https://doi.org/10.1126/science.1553535.
25. Mirpour, K. & Bisley, J.W. (2012). Anticipatory remapping of attentional priority across the entire visual field. *J. Neurosci.* 32, 16449–16457. https://doi.org/10.1523/JNEUROSCI.2008-12.2012.
26. Fabius, J.H., Fracasso, A., Acunzo, D.J., van der Stigchel, S. & Melcher, D. (2020). Low-level visual information is maintained across saccades, allowing for a

postsaccadic handoff between visual areas. *J. Neurosci.* 40, 9476–9486. https://doi.org/10.1523/JNEUROSCI.1169-20.2020.

27. Xiao, W., Sharma, S., Kreiman, G. & Livingstone, M.S. (2024). Feature-selective responses in macaque visual cortex follow eye movements during natural vision. *Nat. Neurosci.* 27, 1157–1166. https://doi.org/10.1038/s41593-024-01631-5.
28. Colby, C.L. & Duhamel, J.-R. (1996). Spatial representations for action in parietal cortex. *Cogn. Brain Res.* 5, 105–115. https://doi.org/10.1016/S0926-6410(96)00046-8.
29. Esteban, O., Markiewicz, C.J., Blair, R.W., Moodie, C.A., Isik, A.I., Erramuzpe, A., Kent, J.D., Goncalves, M., DuPre, E., Snyder, M., et al. (2019). fMRIPrep: A robust preprocessing pipeline for functional MRI. *Nat. Methods* 16, 111–116. https://doi.org/10.1038/s41592-018-0235-4.
30. Jenkinson, M., Beckmann, C.F., Behrens, T.E.J., Woolrich, M.W. & Smith, S.M. (2012). FSL. *NeuroImage* 62, 782–790. https://doi.org/10.1016/j.neuroimage.2011.09.015.
31. Peirce, J., Gray, J.R., Simpson, S., MacAskill, M., Höchenberger, R., Sogo, H., Kastman, E. & Lindeløv, J.K. (2019). PsychoPy2: Experiments in behavior made easy. *Behav. Res. Methods* 51, 195–203. https://doi.org/10.3758/s13428-018-01193-y.
32. Dale, A.M., Fischl, B. & Sereno, M.I. (1999). Cortical surface–based analysis. *NeuroImage* 9, 179–194. https://doi.org/10.1006/nimg.1998.0395.
33. Cox, R.W. (1996). AFNI: Software for analysis and visualization of functional magnetic resonance neuroimages. *Comput. Biomed. Res.* 29, 162–173. https://doi.org/10.1006/cbmr.1996.0014.
34. Pedregosa, F., Varoquaux, G., Gramfort, A., Michel, V., Thirion, B., Grisel, O., Blondel, M., Prettenhofer, P., Weiss, R., Dubourg, V., Vanderplas, J., Passos, A., Cournapeau, D., Brucher, M., Perrot, M. & Duchesnay, E. (2011). Scikit-learn: Machine learning in Python. *J. Mach. Learn. Res.* 12, 2825–2830.
35. Virtanen, P., Gommers, R., Oliphant, T.E., Haberland, M., Reddy, T., Cournapeau, D., Burovski, E., Peterson, P., Weckesser, W., Bright, J., et al. (2020). SciPy 1.0: Fundamental algorithms for scientific computing in Python. *Nat. Methods* 17, 261–272. https://doi.org/10.1038/s41592-019-0686-2.
36. Engbert, R. & Mergenthaler, K. (2006). Microsaccades are triggered by low retinal image slip. *Proc. Natl. Acad. Sci.* 103, 7192–7197. https://doi.org/10.1073/pnas.0509557103.

37. Schweitzer, R. & Rolfs, M. (2022). Definition, Modeling, and Detection of Saccades in the Face of Post-Saccadic Oscillations. In Eye Tracking Neuromethods, S. Stuart, ed. (Springer US), pp. 69–95. https://doi.org/10.1007/978-1-0716-2391-6_5.
38. Baldauf, D. & Deubel, H. (2008). Properties of attentional selection during the preparation of sequential saccades. *Exp. Brain Res.* 184, 411–425. https://doi.org/10.1007/s00221-007-1114-x.
39. Gersch, T.M., Kowler, E. & Dosher, B. (2004). Dynamic allocation of visual attention during the execution of sequences of saccades. *Vision Res.* 44, 1469–1483. https://doi.org/10.1016/j.visres.2003.12.014.
40. Godijn, R. & Theeuwes, J. (2003). Parallel allocation of attention prior to the execution of saccade sequences. *J. Exp. Psychol. Hum. Percept. Perform.* 29, 882–896. https://doi.org/10.1037/0096-1523.29.5.882.